Accepted Manuscript

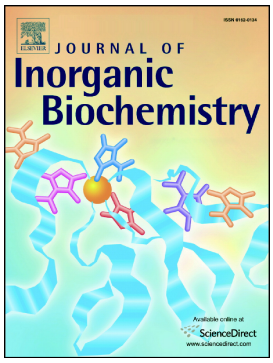

Ruthenium(II) polypyridyl complexes: Synthesis, characterization and anticancer activity studies on BEL-7402 cells

Dan Wan, Shang-Hai Lai, Chuan-Chuan Zeng, Cheng Zhang, Bing Tang, Yun-Jun Liu

PII: S0162-0134(17)30072-7
DOI: doi: 10.1016/j.jinorgbio.2017.04.026
Reference: JIB 10212

To appear in: *Journal of Inorganic Biochemistry*

Received date: 8 February 2017
Revised date: 24 April 2017
Accepted date: 26 April 2017

Please cite this article as: Dan Wan, Shang-Hai Lai, Chuan-Chuan Zeng, Cheng Zhang, Bing Tang, Yun-Jun Liu , Ruthenium(II) polypyridyl complexes: Synthesis, characterization and anticancer activity studies on BEL-7402 cells. The address for the corresponding author was captured as affiliation for all authors. Please check if appropriate. Jib(2017), doi: 10.1016/j.jinorgbio.2017.04.026

This is a PDF file of an unedited manuscript that has been accepted for publication. As a service to our customers we are providing this early version of the manuscript. The manuscript will undergo copyediting, typesetting, and review of the resulting proof before it is published in its final form. Please note that during the production process errors may be discovered which could affect the content, and all legal disclaimers that apply to the journal pertain.

ACCEPTED MANUSCRIPT

Submitted to JIB

Ruthenium (II) polypyridyl complexes: synthesis, characterization and anticancer activity studies on BEL-7402 cells

Dan Wan[a,1], Shang-Hai Lai[a,1], Chuan-Chuan Zeng[a], Cheng Zhang[a], Bing Tang[a], Yun-Jun Liu[a,b,*]

[a]*School of Pharmacy, Guangdong Pharmaceutical University, Guangzhou, 510006, PR China*

[b]*Guangdong Cosmetics Engineering & Technology Research Center, Guangzhou, 510006, PR China*

[1]*These authors contribute equally*

ACCEPTED MANUSCRIPT

* Corresponding author. *E-mail address:* lyjche@163.com(Y.J. Liu).

ACCEPTED MANUSCRIPT

Abstract Two new ligand PTTP (2-phenoxy-1,4,8,9-tetraazatriphenylene) and FTTP (2-(3-fluoronaphthalen-2-yloxy)-1,4,8,9-tetraazatriphenylene) and their six ruthenium(II) polypyridyl complexes $[Ru(N\text{-}N)_2(PTTP)](ClO_4)_2$ and $[Ru(N\text{-}N)_2(FTTP)](ClO_4)_2$ (N-N = dmb: 4,4′-dimethyl-2,2′-bipiridine; dmp: 2,9-dimethyl-1,10-phenanthroline; ttbpy: 4,4′-ditertiarybutyl-2,2′-bipyridine) were synthesized and characterized. The cytotoxic activity of the complexes against cancer cells HeLa, BEL-7402, A549, HepG-2, HOS and normal cell LO2 was evaluated by MTT method. The IC_{50} values range from 1.5 ± 0.1 to 55.9 ± 7.5 μM. Complex **3** shows the highest cytotoxic activity toward BEL-7402 cells (IC_{50} = 1.5 ± 0.1 μM). Complex **5** displays most effective inhibition of the cell growth in A549 and HOS cells with low IC_{50} values of 2.5 ± 0.6 and 2.6 ± 0.1 μM, respectively. The apoptosis, reactive oxygen species, mitochondrial membrane potential, DNA damage, autophagy and anti-metastasis assay were investigated under a fluorescent microscope. The cell cycle arrest was assayed by flow cytometry, and the expression of caspases and Bcl-2 family proteins was studied by western blot. The results obtained show that the complexes induce apoptosis in BEL-7402 cells through a ROS-mediated mitochondrial dysfunction pathway.

Keywords: Ru(II) polypyridyl complexes; apoptosis; anti-metastasis assay; autophagy; ROS; western blot.

ACCEPTED MANUSCRIPT

1. Introduction

Transition metal complexes have received great attention as cancer therapy, due to the clinical sources of cisplatin and its derivatives [1,2]. However, the side-effect of cisplatin such as neurotoxicity and nephrotoxicity [3,4] limited the its clinical application. These drawbacks in platinum-based anticancer drugs have stimulated considerable attempts to replace cisplatin with suitable alternatives by other transition metal complexes. Ruthenium is the most attractive metal owing to its chemical and air stability, structural diversity, low toxicity and ability to mimic iron binding in biological system, which finally supported them as highly potent anticancer agents other than platinum based drugs [5-9]. Recently, ruthenium compounds have received increasing attention in the medicinal chemistry field, especially in relation to the development of chemotherapeutics that present minimal side effects and immunity to the acquisition of drug resistance [10,11]. Presently, ruthenium complex NKP-1339 (*trans*-[tetrachloridobis(1*H*-indazole)ruthenate(III)]) has successfully entered into the clinical trials [12, 13]. NKP-1339 has been studied against solid tumors and showed promising results in a phase I clinical trial, most remarkably in patients with gastrointestinal neuroendocrine tumors [14]. The ruthenium(II) complexes containing dppz-like (dppz = dipyrido[3,2-*a*-2′,3′-*c*]phenanzine) show high anticancer activity. Complex $[Ru(bpy)_2(dppn)]^{2+}$ (dppn = benzo[*i*]dipyrido[3,2-*a*:2′,3′-*h*]quinoxaline) displays high inhibitory effect on the cell growth in HT-29 (IC_{50} = 6.4 ± 1.9 μM) and MCF-7 (IC_{50} = 3.3 ± 1.2 μM) [15]. $[Ru(bpy)(phpy)(dppz)]^{+}$ (phpy = 2-phenylpyridine) was found to be rapidly taken up by cancer cells after a 2 h incubation [16].

ACCEPTED MANUSCRIPT

$[Ru(phpy)(bpy)(dppn)]^+$ (bpy = 2,2′-bipyridine) is 6 times more active than the platinum drug against HeLa cells, and it is able to disrupt the mitochondria membrane potential [17]. $[Ru(phen)_2(addppn)]^{2+}$ (addppn = acenaphtheno[1,2-b]-1,4-diazabenzo[i]dipyrido[3,2-*a*:2′,3′-*c*]phenazine) inhibits the cell growth in BEL-7402 cell (IC_{50} = 3.9 ± 0.4 μM) at G0/G1 phase and G2/M phase in SK-BR-3 cell (IC_{50} = 5.1 ± 0.6 μM) [18]. Ru(II) complex $[Ru(dmp)_2(pddppn)]^{2+}$ (pddppn = phenantheno[1,2-b]-1,4-diazabenzo[i]dipyrido[3,2-*a*:2′,3′-*c*]phenazine) exhibits very high cytotoxic activity toward BEL-7402 (IC_{50} = 1.6 ± 0.4 μM), MG-63 (IC_{50} = 1.5 ± 0.2 μM) and A549 cells (IC_{50} = 1.5 ± 0.3 μM) [19]. Changes in the structure of main ligand could be used to attain diverse anticancer activity of ruthenium(II) complexes. Therefore, extensive studies on different structure dppz-like main ligand are necessary to further elucidate the anticancer effect and mechanism of Ru(II) complexes and discover some new potential anticancer reagents. In this article, two new dppz-like ligands PTTP (PTTP = 2-phenoxy-1,4,8,9-tetraazatriphenylene) and FTTP (FTTP = 2-(3-fluoronaphthalen-2-yloxy)-1,4,8,9-tetraazatriphenylene) and their ruthenium(II) polypyridyl complexes $[Ru(N\text{-}N)_2(PTTP)](ClO_4)_2$ and $[Ru(N\text{-}N)_2(FTTP)](ClO_4)_2$ (N-N = dmb: 4,4′-dimethyl-2,2′-bipiridine; dmp: 2,9-dimethyl-1,10-phenanthroline; ttbpy: 4,4′-ditertiary butyl-2,2′-bipyridine, Scheme 1) were synthesized and characterized by elemental analysis, ESI-MS, IR, ^1H NMR and ^{13}C NMR. The cytotoxicity in vitro, apoptosis, reactive oxygen species, mitochondrial membrane potential, cell cycle distribution, cell invasion, autophagy and Bcl-2 family proteins expression were investigated.

ACCEPTED MANUSCRIPT

2. Experimental

2.1. Materials and methods

All reagents and solvents were purchased commercially and used without further purification unless otherwise noted. Ultrapure MilliQ water was used in all experiments. DMSO, 4,4'-dimethyl-2,2'-bipyridine (dmb), 4,4′-ditertiary butyl-2,2′-bipyridine (ttbpy), 2,9-dimethyl-1,10-phenanthroline (dmp), and RPMI (Roswell Park Memorial Institute) 1640 were purchased from Sigma. 1,10-phenanthroline was obtained from the Guangzhou Chemical Reagent Factory. BEL-7402 (human hepatocellular carcinoma), A549 (human lung carcinoma), HeLa (human cervical cancer), HepG2 (human hepatocellular carcinoma), HOS (human osteosarcoma) and normal LO2 (human liver cancer) cell lines were purchased from the American Type Culture Collection. $RuCl_3 \cdot 3H_2O$ was purchased from the Kunming Institution of Precious Metals.

Microanalysis (C, H, and N) was carried out with a Perkin-Elmer 240Q elemental analyzer. Electrospray ionization mass spectra (ESI-MS) were recorded on a LCQ system (Finnigan MAT, USA) using acetonitrile as mobile phase. The spray voltage, tube lens offset, capillary voltage and capillary temperature were set at 4.50 KV, 30.00 V, 23.00 V and 200 ^{o}C, respectively, and the quoted *m/z* values are for the major peaks in the isotope distribution. ^{1}H NMR and ^{13}C NMR spectra were recorded on a Varian-500 spectrometer with DMSO-d_6 as solvent and tetramethylsilane (TMS) as an internal standard at 500 MHz at room temperature.

ACCEPTED MANUSCRIPT

2.2. Synthesis of ligands and complexes

2.2.1. 2-phenoxy-1,4,8,9-tetraazatriphenylene (PTTP)

1,10-phenthroline-5,6-dione (0.210 g, 1.00 mmol) [20], 4-phenoxybenzene-1,2-diamine (0.200 g, 1.00 mmol) and citric acid (0.035g, 1.82 mmol) were dissolved in 30 mL of ethanol and react at room temperature for 15 min. The brown precipitate was washed with water (3 × 30 mL) and brown powder was obtained. Yield: 85%. Anal. Calcd for $C_{24}H_{14}N_4O$: C, 76.99; H, 3.77; N, 14.96%. Found: C, 76.87; H, 3.86; N, 15.06%. FAB-MS: m/z = 375 [M + 1]. IR (KBr, cm^{-1}): 3373.3, 3056.4, 2964.1, 1626.9, 1599.9, 1509.4, 1453.9, 1437.6, 1404.4, 1358.1, 1323.3, 1222.1, 1159.4, 1071.2, 873.2, 742.8.

2.2.2. 2-(3-fluoronaphthalen-2-yloxy)-1,4,8,9-tetraazatriphenylene (FTTP)

1,10-phenthroline-5,6-dione (0.210 g, 1.00 mmol), 4-(3-fluoronaphthalene-2-yloxy)benzene-1,2-diamine (0.268 g, 1 mmol) and citric acid (0.035g, 1.82 mmol) were dissolved in 30 mL of ethanol and react at room temperature for 15 min. The brown precipitate was washed with water (3 × 30 mL) and brown powder was obtained. Yield: 85%. Anal. Calcd for $C_{28}H_{15}FN_4O$: C, 76.01; H, 3.42; N, 12.66%. Found: C, 75.89; H, 3.55; N, 12.45%. FAB-MS: m/z = 443 [M + 1]. IR (KBr, cm^{-1}): 3391.5, 3045.2, 1720.9, 1619.8, 1586.9, 1481.8, 1407.3, 1360.7, 1257.5, 1169.0, 1071.3, 858.7, 741.2.

ACCEPTED MANUSCRIPT

*2.2.3. Synthesis of [Ru(dmb)$_2$(PTTP)](ClO$_4$)$_2$ (**1**)*

A mixture of cis-[Ru(dmb)$_2$Cl$_2$]·2H$_2$O [21] (0.288 g, 0.50 mmol) and PTTP (0.162 g, 0.50 mmol) in ethylene glycol (20 mL) was refluxed under argon for 8 h to give a clear red solution. Upon cooling, a red precipitate was obtained by dropwise addition of saturated aqueous NaClO$_4$ solution. The crude product was purified by column chromatography on neutral alumina with a mixture of CH$_3$CN-ethanol (4:1, v/v) as eluent. The red band was collected. The solvent was removed under reduced pressure and a red powder was obtained. Yield: 73%. UV/Vis (PBS): λ_{max} (ε) = 284 (68440), 401 (13520), 439 (12480). Anal. Calc for C$_{48}$H$_{38}$N$_8$Cl$_2$O$_9$Ru: C, 55.28; H, 3.67; N, 10.74%. Found: C, 55.41; H, 3.84; N, 10.53%. IR (KBr, cm^{-1}): 3399.9, 3059.3, 2964.5, 1618.6, 1598.8, 1528.6, 1479.9, 1452.8, 1353.0, 1313.5, 1243.8, 1221.8, 1195.3, 1144.7, 821.5, 624.2. ^{1}H NMR (DMSO-d$_6$, Fig. S1a, supporting information): δ 9.56 (d, 2H, *J* = 7.0 Hz), 8.72 (d, 4H, *J* = 8.5 Hz), 8.54 (d, 1H, *J* = 8.5 Hz), 8.22 (dd, 2H, *J* = 5.0, *J* = 5.5 Hz), 8.03 (d, 1H, *J* = 6.5 Hz), 7.99 (d, 1H, *J* = 8.5 Hz), 7.92 (d, 1H, *J* = 8.0 Hz), 7.62 (d, 4H, *J* = 5.5 Hz), 7.54 (t, 2H, *J* = 5.5 Hz), 7.51 (d, 1H, *J* = 3.0 Hz), 7.43-7.37 (m, 5H), 7.19 (d, 2H, *J* = 5.5 Hz), 2.56 (s, 6H), 2.47 (s, 6H). ^{13}C NMR: (DMSO-d$_6$, 125 MHz, ppm): 156.27, 156.05, 153.31, 151.77, 151.01, 150.39, 150.18, 150.07, 149.69, 149.61, 140.46, 139.80, 139.19, 133.89, 132.61, 130.99, 129.78, 128.54, 128.32, 127.94, 127.53, 127.39, 127.13, 126.08, 125.05, 124.97, 120.08, 116.76, 20.75, 20.66. ESI-MS (CH$_3$CN): m/z 422.5 ([M-2ClO$_4$]$^{2+}$).

2.2.4. Synthesis of [Ru(dmp)$_2$(PTTP)](ClO$_4$)$_2$ (2)

ACCEPTED MANUSCRIPT

This complex was synthesized in a manner identical to that described for **1**, with $[Ru(dmp)_2Cl_2]\cdot 2H_2O$ [22] in place of $[Ru(dmb)_2Cl_2]\cdot 2H_2O$. Yield: 72%. UV/Vis (PBS): λ_{max} = 283 (54840), 396 (14800), 435 (12000). Anal. Calc for $C_{52}H_{38}N_8Cl_2O_9Ru$: C, 57.25; H, 3.51; N, 10.27%. Found: C, 57.11; H, 3.71; N, 10.42%. IR (KBr, cm^{-1}): 3481.3, 3057.4, 2923.7, 1624.8, 1597.6, 1509.0, 1480.1, 1462.7, 1354.8, 1314.4, 1244.9, 1222.3, 1195.1, 1162.1, 856.7, 622.8. ^{1}H NMR (DMSO-d_6, Fig. S1b, supporting information): δ 9.38 (d, 2H, *J* = 7.0 Hz), 8.93 (dd, 2H, *J* = 8.0, *J* = 9.0 Hz), 8.46 (d, 4H, *J* = 7.0 Hz), 8.42 (d, 1H, *J* = 4.5 Hz), 8.26 (dd, 2H, *J* = 5.5, *J* = 5.5 Hz), 7.99 (d, 3H, *J* = 5.0 Hz), 7.58 (d, 3H, *J* = 6.5 Hz), 7.54 (d, 1H, *J* = 6.0 Hz), 7.49 (d, 2H, *J* = 5.5 Hz), 7.44 (d, 1H, *J* = 2.5 Hz), 7.41 (d, 1H, *J* = 2.5 Hz), 7.39 (d, 1H, *J* = 3.0 Hz), 7.37 (d, 1H, *J* = 5.0 Hz), 7.34 (d, 1H, *J* = 6.5 Hz), 7.32 (d, 1H, *J* = 2.5 Hz), 1.93 (s, 6H), 1.82 (s, 6H). ^{13}C NMR (DMSO-d6, 125 MHz, ppm): 168.22, 166.95, 154.96, 153.98, 152.02, 151.16, 150.99, 150.89, 148.96, 147.74, 140.51, 139.89, 139.54, 139.31, 138.43, 136.88, 134.05, 133.77, 133.55, 131.19, 129.71, 129.59, 128.14, 127.74, 127.61, 127.39, 127.32, 126.99, 126.70, 126.53, 126.31, 120.16, 116.77, 113.91, 26.17, 25.83, 24.67, 19.05. ESI-MS (CH_3CN): m/z 993.0 ($[M\text{-}ClO_4]^+$), 890.2 ($[M\text{-}2ClO_4\text{-}H]^+$), 446.6 ($[M\text{-}2ClO_4]^{2+}$).

2.2.5. Synthesis of $[Ru(ttbpy)_2(PTTP)](ClO_4)_2$ (3)

This complex was synthesized in a manner identical to that described for **1**, with $[Ru(ttbpy)_2Cl_2]\cdot 2H_2O$ [21] in place of $[Ru(dmb)_2Cl_2]\cdot 2H_2O$. Yield: 70%. UV/Vis (PBS): λ_{max} = 285 (68760), 403 (16160), 437 (15600). Anal. Calc for

ACCEPTED MANUSCRIPT

$C_{60}H_{62}N_8Cl_2O_9Ru$: C, 59.49; H, 5.16; N, 9.26%. Found: C, 59.78; H, 5.08; N, 9.14%. IR (KBr, cm^{-1}): 3500.4, 3072.8, 2958.5, 1614.7, 1540.3, 1509.2, 1480.3, 1462.7, 1413.3, 1362.2, 1314.6, 1245.8, 1222.7, 1194.5, 1161.9, 838.2, 622.3. ^{1}H NMR (DMSO-d_6, Fig. S1c, supporting information): δ 9.58 (d, 2H, *J* = 8.0 Hz), 8.87 (d, 4H, *J* = 8.5 Hz), 8.53 (d, 1H, *J* = 9.0 Hz), 8.14 (d, 2H, *J* = 5.5 Hz), 8.03 (dd, 2H, *J* = 3.5, *J* = 2.5 Hz), 7.97 (d, 1H, *J* = 3.0 Hz), 7.64 (d, 4H, *J* = 6.5 Hz), 7.61 (d, 2H, *J* = 2.5 Hz), 7.59 (d, 2H, *J* = 2.5 Hz), 7.50 (d, 1H, *J* = 2.5 Hz), 7.42 (d, 1H, *J* = 7.5 Hz), 7.38 (d, 4H, *J* = 5.5 Hz), 1.43 (s, 18H), 1.35 (s, 18H). ^{13}C NMR (DMSO-d6, 125 MHz, ppm): 161.94, 161.82, 156.49, 156.28, 153.12, 151.78, 151.26, 151.14, 150.67, 150.22, 150.11, 140.46, 139.84, 139.34, 139.25, 133.89, 132.94, 132.69, 130.99, 129.88, 129.83, 128.88, 128.19, 127.95, 127.69, 127.54, 127.14, 126.08, 124.84, 124.35, 121.90, 121.81, 120.08, 116.76, 114.36, 114.22, 113.67, 35.54, 35.43, 30.08, 29.98. ESI-MS (CH_3CN): m/z 1111.3 ($[M\text{-}ClO_4]^+$, 506.4 ($[M\text{-}2ClO_4]^{2+}$).

2.2.6. Synthesis of $[Ru(dmb)_2(FTTP)](ClO_4)_2$ (4)

This complex was synthesized in a manner identical to that described for **1**, with FTTP in place of PTTP. Yield: 71%. UV/Vis (PBS): λ_{max} = 283 (69000), 390 (13720), 441 (12280). Anal. Calc for $C_{52}H_{39}N_8FCl_2O_9Ru$: C, 56.22; H, 3.54; N, 10.09%. Found: C, 56.34; H, 3.66; N, 10.28%. IR (KBr, cm^{-1}): 3433.4, 3067.0, 2960.3, 1618.4, 1586.9, 1547.3, 1485.8, 1468.7, 1414.7, 1354.9, 1307.5, 1217.4, 1208.6, 1175.8, 819.1, 622.3. ^{1}H NMR (DMSO-d_6, Fig. S1d, supporting information): δ 9.55 (d, 1H, *J* = 7.0 Hz), 9.48 (d, 1H, *J* = 7.0 Hz), 8.72 (dd, 4H, *J* = 5.0, *J* = 5.5 Hz), 8.55 (d, 1H, *J* = 6.0 Hz),

ACCEPTED MANUSCRIPT

8.24 (dd, 2H, *J* = 5.0, *J* = 5.5 Hz), 8.20 (d, 1H, *J* = 5.5 Hz), 8.06 (d, 1H, *J* = 3.0 Hz), 8.01 (d, 1H, *J* = 5.5 Hz), 7.97 (d, 1H, *J* = 6.0 Hz), 7.93 (d, 1H, *J* = 2.5 Hz), 7.88 (d, 1H, *J* = 5.0 Hz), 7.67 (d, 1H, *J* = 8.5 Hz), 7.64-7.58 (m, 5H), 7.53 (dd, 2H, *J* = 6.0, *J* = 5.5 Hz), 7.41 (d, 2H, *J* = 5.0 Hz), 7.19 (d, 2H, *J* = 6.0 Hz), 2.54 (s, 6H), 2.46 (s, 6H). ^{13}C NMR (DMSO-d6, 125 MHz, ppm): 160.89, 156.29, 156.06, 154.26, 153.38, 153.03, 151.03, 150.40, 149.91, 149.68, 149.59, 143.25, 140.32, 139.03, 138.52, 133.03, 132.54, 131.58, 130.76, 130.07, 129.81, 128.54, 128.33, 127.54, 127.40, 126.26, 125.86, 125.05, 124.97, 120.91, 110.49, 20.76, 20.67. ESI-MS (CH_3CN): m/z 1013.0 ($[M\text{-}ClO_4]^+$), 456.5 ($[M\text{-}2ClO_4]^{2+}$).

2.2.7. Synthesis of $[Ru(dmp)_2(FTTP)](ClO_4)_2$ (5)

This complex was synthesized in a manner identical to that described for **2**, with FTTP in place of PTTP. Yield: 72%. UV/Vis (PBS): λ_{max} = 270 (58240), 389 (15080), 451 (10400). Anal. Calc for $C_{56}H_{39}N_8FCl_2O_9Ru$: C, 58.04; H, 3.39; N, 9.67%. Found: C, 58.25; H, 3.31; N, 9.78%. IR (KBr, cm^{-1}): 3400.6, 3069.3, 2923.6, 1623.2, 1587.7, 1487.3, 1469.9, 1447.6, 1358.3, 1307.9, 1236.3, 1217.6, 1203.5, 860.7, 624.3. ^{1}H NMR (DMSO-d_6, Fig. S1e, supporting information): δ 9.37 (d, 2H, *J* = 7.0), 8.90 (t, 2H, *J* = 7.5 Hz), 8.46 (d, 4H, *J* = 8.5 Hz), 8.41 (d, 1H, *J* = 4.5 Hz), 8.24 (dd, 2H, *J* = 8.5, *J* = 8.5 Hz), 8.15 (d, 1H, *J* = 8.5 Hz), 8.04 (d, 1H, *J* = 2.0 Hz), 7.95 (d, 3H, *J* = 6.5 Hz), 7.86 (d, 1H, *J* = 2.5 Hz), 7.63-7.57 (m, 6H), 7.51 (d, 1H, *J* = 1.0 Hz), 7.46 (d, 1H, *J* = 1.5 Hz), 7.39 (dd, 2H, *J* = 5.0, *J* = 5.0 Hz), 1.91 (s, 6H), 1.81 (s, 6H). ^{13}C NMR (DMSO-d6, 125 MHz, ppm): 167.99, 166.79, 160.69, 154.32, 153.78, 153.47,

ACCEPTED MANUSCRIPT

151.05, 150.59, 148.79, 147.55, 143.09, 140.31, 138.87, 138.55, 138.21, 136.64, 133.66, 133.16, 131.42, 130.71, 129.71, 129.52, 129.45, 127.52, 127.40, 127.13, 126.83, 126.46, 126.31, 126.09, 125.77, 120.77, 110.58, 25.98, 24.49. ESI-MS (CH_3CN): m/z 480.1 ($[M-2ClO_4]^{2+}$).

2.2.8. Synthesis of $[Ru(ttbpy)_2(FTTP)](ClO_4)_2$ (6)

This complex was synthesized in a manner identical to that described for **3**, with FTTP in place of PTTP. Yield: 71%. UV/Vis (PBS): λ_{max} = 290 (58560), 391 (19200), 442 (17080). Anal. Calc for $C_{64}H_{63}N_8FCl_2O_9Ru$: C, 60.09; H, 4.96; N, 8.76%. Found: C, 60.27; H, 4.74; N, 8.89%. IR (KBr, cm^{-1}): 3489.2, 3072.4, 2906.9, 1615.2, 1588.2, 1541.5, 1486.2, 1469.2, 1414.1, 1366.8, 1308.6, 1237.2, 1219.1, 1208.7, 1176.9, 1156.9, 843.5, 622.8. ^{1}H NMR (DMSO-d_6, Fig. S1f, supporting information): δ 9.57 (d, 1H, *J* = 7.0 Hz), 9.51 (d, 1H, *J* = 7.5 Hz), 8.87 (d, 4H, *J* = 7.5 Hz), 8.55 (d, 1H, *J* = 6.5 Hz), 8.17 (d, 2H, *J* = 5.5 Hz), 8.14 (d, 1H, *J* = 5.0 Hz), 8.07 (d, 2H, *J* = 5.5 Hz), 7.99 (d, 1H, *J* = 2.0 Hz), 7.93 (d, 2H, *J* = 5.5 Hz), 7.68 (d, 1H, *J* = 9.0 Hz), 7.65-7.59 (m, 7H), 7.37 (d, 2H, *J* = 5.0 Hz), 7.26 (d, 1H, *J* = 1.5 Hz), 7.18 (d, 1H, *J* = 2.0 Hz), 1.43 (s, 18H), 1.33 (s, 18H). ^{13}C NMR (DMSO-d6, 125 MHz, ppm): 161.95, 161.82, 160.92, 156.51, 156.29, 154.27, 153.21, 152.86, 151.29, 150.69, 150.42, 149.96, 143.28, 140.39, 139.05, 138.59, 133.13, 132.64, 131.60, 130.77, 130.18, 129.91, 127.66, 127.51, 126.26, 125.88, 124.85, 124.37, 121.91, 121.82, 120.93, 110.53, 35.55, 35.43, 30.08, 29.98. ESI-MS (CH_3CN): m/z 1179.1 ($[M-ClO_4]^+$), 540.2 ($[M-2ClO_4]^{2+}$).

ACCEPTED MANUSCRIPT

2.3. Stability of the complexes in buffer

All the complexes were first dissolved in a minimum amount of DMSO (0.5% of the final volume) and then diluted with PBS to a required concentration. The stability was analyzed by monitoring the electronic spectra over 48 h on a Shimadzu MPS-2000 spectrophotometer.

2.4. Cytotoxic activity evaluation in vitro

3-(4,5-dimethylthiazole)-2,5-diphenyltetraazolium bromide (MTT) method [23] was used to determine the cytotoxic activity in vitro of the complexes. Cells were placed in 96-well microassay culture plates (8×10^3 cells per well) and grown overnight at 37 °C in a 5% CO_2 incubator. The tested complexes were dissolved in DMSO and then added to the wells to achieve final concentrations ranging from 10^{-6} to 10^{-4} M. Control wells were prepared by addition of culture medium (100 μL). The plates were incubated at 37 °C in a 5% CO_2 incubator for 48 h. Upon completion of the incubation, stock MTT dye solution (20 μL, 5 mg/mL^{-1}) was added to each well. After 4 h, buffer (100 μL) containing dimethylformamide (50%) and sodium dodecyl sulfate (20%) was added to solubilize the MTT formazan. The optical density of each well was measured with a microplate spectrophotometer at a wavelength of 490 nm. The IC_{50} values were determined by the percentage of cell viability versus concentration on a logarithmic graph and reading off the concentration at which 50% of cells remain viable relative to the control. Each experiment was repeated at least

ACCEPTED MANUSCRIPT

three times to obtain the mean values.

2.5. Apoptosis assay by AO/EB staining method

BEL-7402 cells were seeded onto chamber slides in six-well plates at a density of 2×10^5 cells per well and incubated for 24 h. The cancer cells were cultured in RPMI 1640 and normal cell LO2 was cultured in DMEM supplemented with 10% of fetal bovine serum (FBS) and incubated at 37 °C in 5% CO_2. The medium was removed and replaced with medium (final DMSO concentration, 0.05% v/v) containing the complexes (6.25 μM) for 24 h. The medium was removed again, and the cells were washed with ice-cold phosphate buffer saline (PBS), and fixed with formalin (4%, w/v). Cell nuclei were counterstained with acridine orange (AO) and ethidium bromide (EB) (AO: 100 μg/mL, EB: 100 μg/mL) for 10 min. The cells were observed and imaged under an inverted fluorescence microscope (Nikon, Yokohama, Japan) with excitation at 350 nm and emission at 460 nm.

2.6. DNA damage assay

DNA damage was investigated by means of comet assay. BEL-7402 cells in culture medium were incubated with 6.25 μM of complexes **1**-**6** for 24 h at 37 °C. The cells were harvested by a trypsinization process at 24 h. A total of 100 μL of 0.5% normal agarose in PBS was dropped gently onto a fully frosted microslide, covered immediately with a coverslip, and then placed at 4 ^{o}C for 10 min. The coverslip was removed after the gel had been set. A mixture of 50 μL of the cell suspension (200

ACCEPTED MANUSCRIPT

cells / μL) mixed with 50 μL of 1% low melting agarose was preserved at 37 °C. A total of 100 μL of this mixture was applied quickly on top of the gel, coated over the microslide, covered immediately with a coverslip, and then placed at 4 ^{o}C for 10 min. The coverslip was again removed after the gel had been set. A third coating of 50 μL of 0.5% low melting agarose was placed on the gel and allowed to place at 4 ^{o}C for 15 min. After solidification of the agarose, the coverslips were removed, and the slides were immersed in an ice-cold lysis solution (2.5 M NaCl, 100 mM EDTA, 10 mM Tris, 90 mM sodium sarcosinate, NaOH, pH 10, 1% Triton X-100 and 10% DMSO) and placed in a refrigerator at 4 °C for 2 h. All of the above operations were performed under low lighting conditions to avoid additional DNA damage. The slides, after removal from the lysis solution, were placed horizontally in an electrophoresis chamber. The reservoirs were filled with an electrophoresis buffer (300 mM NaOH, 1.2 mM EDTA) until the slides were just immersed in it, and the DNA was allowed to unwind for 30 min in electrophoresis solution. Then the electrophoresis was carried out at 25 V and 300 mA for 20 min. After electrophoresis, the slides were removed, washed thrice in a neutralization buffer (400 mM Tris, HCl, pH 7.5). Cells were stained with 20 μL of EB (20 μg·mL^{-1}) in the dark for 20 min. The slides were washed in cold distilled water for 10 min to neutralize the excess alkali, air-dried and imaged under an inverted fluorescent microscope.

2.7. Reactive oxygen species (ROS) detection

BEL-7402 cells were seeded into six-well plates (Costar, Corning Corp, New

ACCEPTED MANUSCRIPT

York) at a density of 2×10^5 cells per well and incubated for 24 h. The cells were cultured in RPMI 1640 supplemented with 10% of FBS and incubated at 37 °C in 5% CO_2. The medium was removed and replaced with medium (final DMSO concentration, 0.05% v/v) containing complexes **1-6** (6.25 μM) for 24 h. The medium was removed again. The fluorescent dye DCHF-DA (10 μM) was added to the medium to cover the cells. The treated cells were then washed with cold PBS-EDTA (EDTA = ethylene diamine tetraacetic acid) twice, collected by trypsinization and centrifugation at 1,500 rpm for 5 min, the cell pellets were suspended in PBS-EDTA and imaged under a fluorescent microscope. The DCF fluorescent intensity was determined by flow cytometry with excitation at 450 nm and emission at 520 nm.

2.8. Mitochondrial membrane potential assay

BEL-7402 cells were treated with the complexes (6.25 μM) in 12-well plates for 24 h and then washed three times with cold PBS. The cells were detached with trypsin-EDTA solution. The collected cells were incubated for 20 min with 1 μg/mL of JC-1 in culture medium at 37 °C in the dark. The cells were immediately centrifuged to remove the supernatant, and the cell pellets were suspended in PBS and imaged under fluorescence microscope. The ratio of red/green fluorescence was determined by FACSCalibur flow cytometry with excitation at 490 nm and emission at 527 nm.

2.9. Cell cycle arrest by flow cytometry

ACCEPTED MANUSCRIPT

BEL-7402 cells were seeded into six-well plates (Costar, Corning Corp, New York) at a density of 2×10^5 cells per well and incubated for 24 h. The cells were cultured in RPMI 1640 supplemented with 10% of FBS and incubated at 37 °C in 5% CO_2. The medium was removed and replaced with medium (final DMSO concentration, 0.05% v/v) containing complexes **1-6** (6.25 μM). After incubation for 24 h, the cell layer was trypsinized and washed with cold PBS and fixed with 70% ethanol. Twenty μL of RNAse (0.2 mg / mL) and 20 μL of propidium iodide (PI, 0.02 mg / mL) were added to the cell suspensions and they were incubated at 37 °C for 30 min. Then the samples were analyzed with a FACSCalibur flow cytometry. The number of cells analyzed for each sample was 10000 [24].

2.10. Matrigel invasion assay

The BD Matrigel invasion chamber was used to investigate the cell invasion according to the manufacturer's instructions. BEL-7402 cells (4×10^4) in serum free media and the complexes (6.25 μM) were seeded in the top chamber of the two chamber Matrigel system. RPMI-1640 (20% FBS) was added as chemo-attractant into the low chamber, and the cells were allowed to invade for 24 h. Then the non-invading cells were removed from the upper surface and cells on the lower surface were fixed with 4% paraformaldehyde and stained with 0.1% of crystal violet. The membranes were photographed and the invading cells were counted under a light microscope. The mean values were obtained from three independent experiments.

ACCEPTED MANUSCRIPT

2.11. Autophagy assay

BEL-7402 cells were seeded onto chamber slides in 12-well plates and incubated for 24 h. The cells were cultured in RPMI 1640 supplemented with 10% of FBS and incubated at 37 ^{o}C in 5% CO_2. The medium was removed and replaced with medium (final DMSO concentration, 0.05% v/v) containing complexes **1**-**6** (6.25 μM) for 24 h. The medium was removed again, and the cells were washed with ice-cold PBS twice. The cells were stained with monodansylcadaverine (MDC) solution (50 μM) for 10 min and washed with PBS twice. Then the cells were observed and imaged under fluorescence microscope. The effect of the complexes on the expression of LC3 and Beclin-1 proteins was assayed by western blot (Bio-rad, Trans-Blot® Turbo™ System).

2.12. The effect of autophagy on cell viability

The cell viability was determined using the MTT method. BEL-7402 cells were placed in 96-well microassay culture plates (8×10^4 cells per well) and cultured overnight at 37 ^{o}C in a 5% CO_2 incubator. The cells were pretreated with 3-methyladenine (3-MA) for 3 h, followed by ruthenium complexes for 24 h. After incubation, the cells were incubated with MTT (0.5 mg/ml) for 4 h at 37 ^{o}C. Upon completion of the incubation, 100 μL DMSO was added to solubilize the MTT formazan. The optical density of each well was then measured with a microplate spectrophotometer at a wavelength of 490 nm. The viability (%) of cell growth was calculated by the formula: $(A_{490\ (treatment\ group)} / A_{490\ (control)}) \times 100$, $A_{490\ (treatment\ group)}$ is

ACCEPTED MANUSCRIPT

the mean OD value of cells treated with the various ruthenium complexes and $A_{490\ (control)}$ is the mean OD value of untreated cells. Each experiment was repeated at least three times to obtain the mean values.

2.13. The expression of caspases and Bcl-2 family proteins

BEL-7402 cells were seeded in 3.5 cm dishes for 24 h and incubated with 6.25 μM of the complexes in the presence of 10% FBS. The cells were harvested in lysis buffer. After sonication, the samples were centrifuged for 20 min at 13,000 g. The protein concentration of the supernatant was determined by BCA (bicinchoninic acid) assay. Sodium dodecyl sulfate-polyacrylamide gel electrophoresis was done loading equal amount of proteins per lane. Gels were then transferred to poly (vinylidene difluoride) membranes (Millipore) and blocked with 5% non-fat milk in TBST [20 mM Tris–HCl, 150 mM NaCl, 0.05% Tween (polyoxyethy-lene monolaurate sorbaitan) 20, pH 8.0) buffer for 1 h. Then the membranes were incubated with primary antibodies at 1:5,000 dilutions in 5% non-fat milk overnight at 4 °C, and washed four times with TBST for a total of 30 min. After which the secondary antibodies conjugated with horseradish peroxidase at 1:5,000 dilution for 1 h at room temperature and then were washed four times with TBST. The blots were visualized with the Amersham ECL Plus western blotting detection reagents according to the manufacturer's instructions. To assess the presence of comparable amount of proteins in each lane, the membranes were stripped finally to detect the β-actin. The gray values were calculated with Bandscan.

ACCEPTED MANUSCRIPT

3. Results and discussion

3.1. Synthesis and characterization

The ligands PTTP and FTTP were synthesized by the reaction of 1,10-phenanthroline-5,6-dione with 4-phenoxybenzene-1,2-diamine or 4-(3-fluoronaphthalene-2-yloxy)benzene-1,2-diamine in ethanol using citric acid as catalyst at room for 15 min. The yellow ligands were obtained by filtration and washed with water (3 × 30 mL). The complexes **1**-**6** were prepared by direct reaction of PTTP or FTTP with appropriate precursor complexes in ethylene glycol in relatively high yield. The desired Ru(II) complexes were isolated as the perchlorates and purified by column chromatography. In the electrospray ionization mass spectra of the complexes, the signals of $[M\text{-}ClO_4]^+$ and $[M\text{-}2ClO_4]^{2+}$ were observed. The observed molecular weights are consistent with the expected values. In the ^{13}C NMR spectra, the chemical shift values of 20.75, 20.66 for **1**, 26.17, 25.83, 24.67, 19.05 for **2**, 30.08, 29.98 for **3**, 20.76, 20.67 for **4**, 25.98, 24.49 for **5** and 30.08, 29.98 for **6** are assigned to methyl group, 35.54, 35.43 for **3** and 35.55, 35.43 for **6** are attributed to the tertiary butyl carbon atoms.

3.2. Stability studies of the complexes in PBS solution

The stability of the complexes in phosphate buffer solution (PBS) was investigated by UV-Vis spectra. As shown in Fig. S2 (supporting information), no obvious changes in absorption of the complex **1** were observed at 0 and 48 h (data not

ACCEPTED MANUSCRIPT

presented for complexes **2**-**6**), which indicated that the complexes are stable in PBS solution.

3.3. Cytotoxic activity assay of the complexes toward cancer cells

The MTT assay was used to evaluate the effects of the complexes **1**-**6** on cytotoxic activity against cancer cells BEL-7402, A549, HeLa, HepG2, HOS and normal LO2 cell lines. Cisplatin was used as a positive control. As shown in Table 1, the IC_{50} values range from 1.5 ± 0.1 to 55.9 ± 7.5 μM. As a whole, the complexes **1**-**6** show different inhibitory effect on the cell growth of the above selected cancer cell lines. Complex **2** displays the highest cytotoxic activity against HeLa and HepG2 cells with low IC_{50} values of 4.1 ± 0.3 and 2.0 ± 0.2 μM, respectively. According to the IC_{50} values, we infer that the ruthenium(II) polypyridyl complexes containing dmp or ttbpy as ancillary ligands reveal higher cytotoxic activity than those complexes with dmb as ancillary ligand. This may be caused by different hydrophobicity, in general, ancillary ligands dmp or ttbpy has larger hydrophobicity than dmb. Complex **3** is the most effect on BEL-7402 cell growth among the complexes, and complex **5** is sensitive to A549 with a low IC_{50} value of 2.5 ± 0.6 μM. Comparing the IC_{50} values, complex **2** exhibits higher cytotoxicity than cisplatin against HeLa, BEL-7402 and HepG2 cells, and complex **5** shows more effective inhibition on the cell growth of A549 and HepG2 cells than cisplatin under the identical conditions. Comparing the cytotoxicity in vitro, adding a benzene ring and a fluorine atom in the complexes **1**-**3**, complexes **4**-**6** show relative lower cytotoxic activity than those of complexes **1**-**3**

ACCEPTED MANUSCRIPT

against BEL-7402 cells. The cytotoxic activity of complexes **2** and **3** against BEL-7402 cells is comparable to those of $[Ru(dmp)_2(pddppn)]^{2+}$ (IC_{50} = 1.6 ± 0.4 μM) [19], $[Ru(dmp)_2(dptbt)]^{2+}$ (dptbt = 12-(2,3-diphenyl-quinoxalin-6-yl)-4,5,10,13-tetraazabenzo[b]triphenylene, IC_{50} = 1.9 ± 0.3 μM) [25]. Regretfully, we found that the complexes **1**-**6** also show high cytotoxic activity against the normal cell line LO2. Therefore, it is very difficult to find a drug only to kill the cancer cells not to kill the normal cells. Since the complexes displayed relative high effect on BEL-7402 cell growth, this cell line was selected for further investigation of the underlying mechanisms accounting for the action of ruthenium complexes.

3.4. Apoptosis studies with AO/EB staining method

External aggression by a chemical compound sensed by the cells causes them to undergo two major forms of death, necrosis or apoptosis, each with very distinct characteristics. The apoptosis of BEL-7402 cells was investigated with acridine orange (AO) and ethidium bromide (EB) double staining method. The AO/EB staining is sensitive to DNA and was used to access changes in nuclear morphology. As shown in Fig. 1, in the control (a), the living cells were stained bright green in spots. After BEL-7402 cells were exposed to 6.25 μM of complexes **1** (b), **2** (c), **3** (d), **4** (e), **5** (f) and **6** (g) for 24 h, green apoptotic cells containing apoptotic features such as nuclear shrinkage, chromatin condensation were found. Similar results can be observed in other ruthenium (II) complexes [26,27]. To quantitatively compare to

ACCEPTED MANUSCRIPT

apoptotic effect induced by the complexes on BEL-7402 cells, the apoptosis was assayed by flow cytometry. In the control (Fig. S3, supporting information), the percentage in the apoptotic cells is 1.03%. After the treatment of the cells with 6.25 μM of complexes **1** (b), **2** (c), **3** (d), **4** (e), **5** (f) and **6** (g) for 24 h, the percentages of apoptotic cells are 15.25%, 13.34%, 6.39%, 6.50%, 9.26% and 3.66%, respectively. The apoptotic effect of complexes **1** and **2** is higher than that of complexes $[Ru(phen)_2(addppn)]^{2+}$ [18]. The apoptotic effect follows the order of **1** > **2** > **5** > **4** > **3** > **6**. This may be caused by the different structures of the complexes. The apoptotic effect is not consistent with the cytotoxic activity of the complexes against BEL-7402 cells (**3** > **2** > **6** > **5** > **4** > **1**). These data suggest that the complexes can induce apoptosis in BEL-7402 cells.

3.5. DNA damage studies

The proliferation of cancer cells needs DNA replication. DNA damage is a useful method to inhibit DNA replication. Moreover, DNA damage leads to DNA fragmentation, which is a hallmark of apoptosis, mitotic catastrophe or both [28]. To investigate the effect of complexes **1**-**6** on the DNA damage, the single cell gel electrophoresis assay known as comet assay was performed to asses DNA integrity. In the control (Fig. 2 (a)), BEL-7402 cells didn′t show comet-like appearance. Treatment of the cell with 6.25 μM of complexes **1** (b), **2** (c), **3** (d), **4** (e), **5** (f) and **6** (g) for 24 h led to a formation with statistically significant and well-formed comets, and the length of the comet tail represents the extent of DNA damage. The results indicate that the

ACCEPTED MANUSCRIPT

complexes can induce DNA damage, which is further evidence of apoptosis.

3.6. Reactive oxygen species (ROS) levels assay

Reactive oxygen species (ROS), including superoxide anion, hydrogen peroxide and hydroxyl radical, have been involved in the actions of many anticancer drugs through initiation of various apoptotic signaling pathways during chemotherapy [29]. Reactive oxygen species (ROS) are known to affect mitochondrial membrane potential and trigger a series of mitochondria associated events including apoptosis [30]. Many literatures reported that ruthenium complexes induce apoptosis through the production of ROS [31-33]. The ROS levels induced by the complexes was evaluated using 2′,7′-dichlorodihydrofluorescein diacetate (DCHF-DA) as fluorescence probe. DCFH-DA is cleaved by intracellular esterases into its non-fluorescent form 2′,7′-Dichloro-3,6-fluorandiol (DCFH). Then the non-fluorescent substrate is oxidized by intracellular free radicals to produce a fluorescent product dichlorofluorescein (DCF) [34,35]. As is shown in Fig. 3A (a), in the control, owing to low ROS levels, it is difficult for DCHF-DA to be transferred into fluorescent product DCF, no obvious fluorescence image spots are observed. BEL-7402 cells exposure to Rosup (b, positive control) and 6.25 μM of complexes **1** (c), **2** (d), **3** (e), **4** (f), **5** (g), **6** (h) for 24 h, a lot of bright green image spots are found. The findings show that the complexes can increase the ROS levels. This reveals that the complexes 1-6, which selectively accumulates in carcinoma mitochondria, activates the ROS-generating machinery and generates the highest amount of ROS

ACCEPTED MANUSCRIPT

when treated with cancer cells, leading to apoptosis. To quantitatively compare the efficiency of ROS levels, DCF fluorescent intensity was determined by flow cytometry. Fig. 3B shows that the DCF fluorescent intensity increases 1.5 for **1**, 1.4 for **2**, 3.3 for **3**, 1.6 for **4**, 1.7 for **5** and 11.4 times for **6** than the original, respectively. The DCF fluorescent intensity increase follows the order of **6** > **3** > **5** > **4** > **1** > **2**. Complexes **6** and **3** show higher effect on the increasing the ROS levels than complexes **1**, **2**, **4** and **5**. This may be caused by substituent tertiary butyl group in **3** and **6**. Comparing the cytotoxicity in vitro, ROS generation induced by complexes **1**-**6** is not in line with the order of cytotoxicity of the complexes against BEL-7402 cells.

3.7. The changes assay in the mitochondrial membrane potential

Mitochondria act as a point of integration for apoptotic signals originating from both extrinsic and intrinsic apoptotic pathways [36,37]. Since ROS production is closely related to mitochondrial dysfunction [38], the changes in mitochondrial membrane potential associated with apoptosis were assayed using 5,5′,6,6′-tetrachloro-1,1′,3,3′-tetrethylbenzimidalylcarbocyanine iodide (JC-1) as fluorescent probe. JC-1 exhibits potential-dependent accumulation in mitochondria, indicated by a fluorescence emission shift from red (~590 nm) to green (~525 nm) [39]. As shown in Fig. 4A (a), JC-1 forms aggregates and emits a red fluorescence corresponding to high mitochondrial membrane potential. After the treatment of BEL-7402 cells with 50 mM cccp (b, carbonyl cyanide 3-chlorophenylhydrazone, positive control) and 6.25 μM of complexes **1** (c), **2** (d), **3** (e), **4** (f), **5** (g) and **6** (h) for

ACCEPTED MANUSCRIPT

24 h, JC-1 forms monomer and emits green fluorescence corresponding to low mitochondrial membrane potential. The changes from the red to the green fluorescence suggest that the complexes cause a decrease in the mitochondrial membrane potential. The changes were also determined by the ratio of red/green fluorescent intensity by flow cytometry. In the control (Fig. 4B), the ratio of red/green fluorescence is 86.6. After BEL-7402 cells were exposed to 6.25 μM of complexes **1**-**6** for 24 h, the ratios of the red/green fluorescence are 7.7, 5.6, 66.5, 14.5, 13.6 and 44.3, respectively. The reduction in the ratio of red/green indicates that the red fluorescence decreases and the green fluorescent intensity increases. The decrease in the mitochondrial membrane potential induced by **1**-**6** follows the order of **2** > **1** > **5** > **4** > **6** > **3**. Complex **2** shows the highest efficiency among the complexes in inducing a decrease in the mitochondrial membrane potential, complexes **3** and **6** exhibit relative lower effect on the mitochondrial membrane potential than other complexes. However, in the assay of ROS levels, complexes **6** and **3** show the highest efficiency on the ROS levels among the complexes. This demonstrates that the complexes cause the order of changes in ROS levels is not consistent with the order of changes in mitochondrial membrane potential. These results reveal that the complexes induced apoptosis in BEL-7402 cells through mitochondria-mediated pathways.

3.8. The cell cycle arrest studies

To further investigate the inhibitory mechanism of the complexes against BEL-7402 cell growth, the cell cycle distribution was studied by flow cytometry. As

ACCEPTED MANUSCRIPT

shown in Fig. 5, in the control, the percentage in the cell at G2/M phase is 15.64%. After the cells were exposed to 6.25 μM of complexes **1**-**6** for 24 h, the percentages in the cell at G2/M phase are 21.13% for **1**, 25.44% for **2**, 19.41% for **3**, 18.64% for **4**, 20.40% for **5** and 19.97% for **6**, respectively. An increase of 5.49% for **1**, 9.80% for **2**, 3.77% for **3**, 3.00% for **4**, 4.76% for **5** and 4.33% for **6** in the percentage in the cell at G2/M phase was observed, accompanied by corresponding reduction in the percentage in the cell at G0/G1 phase. The data indicate that the complexes inhibit the cell growth in BEL-7402 cells at G2/M phase. Further the analyses find that the effect of the complexes on the cell cycle arrest follows the order of **2** > **1** > **5** > **6** > **3** > **4**. Thus, it can be seen that the cytotoxic activity of the complexes has no inevitable connection with the effect on the cell cycle arrest.

3.9. Matrigel invasion assay

As a confirmatory test, the anti-invasive potential of the complexes towards BEL-7402 cells in the matrigel assay was evaluated. The results obtained from the study are shown in Table 2 and Table 3. In the presence of 6.25 μM of the complexes **1**-**6**, the number of cell invasion decreased. Complexes **1**-**6** inhibiting the percentage of cell invasion are 21.2%, 20.1%, 21.5%, 25.3%, 71.9% and 33.6% invasion, respectively. The anti-metastatic effect of the complexes against BEL-7402 cells followed the order of **6** > **5** > **4** > **3** > **1** > **2**, this is not consistent with cytotoxic activity of the complexes. To evaluate the effect of concentration on the cell invasion, BEL-7402 cells were treated with different concentration of complex **6**. As shown in

ACCEPTED MANUSCRIPT

Table 3, BEL-7402 cells were exposed to 6.25 μM of complex **6**, the percentage of inhibiting invasion cell is 33.6%. When the concentration of **6** is 50.0 μM, the percentage of inhibiting invasion cell reaches 58.5%. Obviously, complex **6** shows a concentration-dependent manner in the inhibiting invasion cell. These results demonstrate that the complexes can effectively inhibit BEL-7402 cell invasion.

3.10. Autophagy induced by the complexes

Autophagy is a life phenomenon and exists extensively in the eucell, and autophagy has been considered to be a third mode of cell death besides apoptosis and necrosis. To determine whether or not autophagy is truly triggered by the complexes, BEL-7402 cells were treated with 6.25 μM of complexes **3** and **6** for 24 h, and the cells were stained with monodansylcadaverine (MDC) as fluorescent probe to detect autophagic activity. As shown in Fig. 6A, compared with the control group, the number of MDC-positive cells in BEL-7402 increased in the complexes-treated cells after 24 h incubation. LC3 is a hallmark, the conversion of LC3-I to LC3-II exhibits autophagy induction [40]. In addition, Beclin-1 protein is necessary to form autophagosomes in autophagy. As shown in Fig. 6B, compared with the control, the expression of LC3-II and Beclin-1 was increased. Comparing the effect of the complexes on the expression of Beclin-1, complex **1** shows the highest autophagic efficiency among the complexes. To investigate the effect of the autophagy on the cell viability, BEL-7402 cells were treated by different concentrations of the complexes in the presence or absence of autophagic inhibitor 3-MA. As shown in Fig. S4

ACCEPTED MANUSCRIPT

(supporting information), compared with the control, the cell viability caused by complexes **3** and **6** decreases in the presence of 3-MA, which indicates that the autophagy inhibits the cell death. The effect of the complexes on autophagy is not consistent with the cytotoxic activity in vitro of the complexes against BEL-7402 cells.

3.11. The expression of caspases and Bcl-2 family proteins studies

Caspases are known to mediate the apoptotic pathway [41,42]. Caspase 3 and 7 are executioners of apoptosis as the processing of their substrates leads to morphological changes associated with apoptosis [43]. The activation of caspase 3 and 7 induced by the complexes was assayed by western blotting. The expression was calculated by the ratio of the expression induced by the complexes/the expression in the control. As shown in Fig. 7, the expression of caspase 3 was upregulated, whereas the level of expression of caspase 7 was downregulated. Bcl-2-related proteins are key regulators of the mitochondria-mediated apoptosis [44]. To further evaluate the effect of the complexes on the expression of Bcl-2 family proteins, BEL-7402 cells were treated with 6.25 μM of complexes **1**-**6** for 24 h. As expected, the expression levels of antiapoptotic proteins Bcl-2 and Bcl-x decreased, whereas the expression of proapoptotic proteins Bak and Bid increased. As a result of these changes, the ratios of Bcl-2/Bak and Bcl-x/Bid decreases significantly, leading to a generation of ROS, a depletion of $\Delta\psi_m$. Subsequently, the complexes induce activation of caspases 3 and 7. All these findings indicate that mitochondrial pathways were involved in apoptosis

ACCEPTED MANUSCRIPT

driven by the complexes.

4. Conclusions

Two new ligands PTTP, FTTP and their six ruthenium(II) complexes were synthesized and characterized in detail. These complexes show relative high anticancer activity against the selected cell lines. Particularly, complex **2** displays strong inhibition of the cell growth toward HeLa, BEL-7402 and HepG-2 cells. Complexes **1**-**6** can enhance the levels of ROS and induce a decrease in the mitochondrial membrane potential, and the complexes inhibit the cell growth in BEL-7402 cells at G2/M phase. In addition, the complexes can induce autophagy and restrain the cell invasion with a concentration-dependent manner and regulate the Bcl-2 family proteins. In summary, the complexes induce apoptosis in BEL-7402 cell through an intrinsic ROS-mediated mitochondrial dysfunction pathway, which was accompanied by the regulation of the expression of Bcl-2 family proteins. In addition, we also conclude that the complexes with high cytotoxicity in vitro against cancer cell may show low effect on ROS, mitochondrial membrane potential and other bioactivity. In summary, we found that the ruthenium (II) complexes containing dmp or ttbpy as ancillary ligands will effectively inhibit cancer cell growth. This work will be helpful for design and synthesis of ruthenium (II) as potent anticancer drugs.

Acknowledgments

This work was supported by the Natural Science foundation of Guangdong

ACCEPTED MANUSCRIPT

Province (No. 2016A030313728), the National Nature Science Foundation of China (No. 81403111) and the Project of innovation for enhancing Guangdong Pharmaceutical University, provincial experimental teaching demonstration center of chemistry & chemical engineering.

ACCEPTED MANUSCRIPT

ACCEPTED MANUSCRIPT

References

[1] L.R. Kelland, N.P. Farell, S. Spinelli, in Uses of Inorganic Chemistry in Medicine, ed. N. P. Farrell, *RSC*, Cambridge, 1999, 109.

[2] B. Rosenberg, L. Vancamp, J. E. Trosko and V. H. Mansour, Nature, 222 (1969) 385-386.

[3] M. Markman, Expert Opin. Drug Saf. 2 (2003) 597–607.

[4] P.C. Bruijninc, P.J. Sadler, Curr. Opin. Chem. Biol. 12 (2008) 197–206.

[5] A.C. Komor, J.K. Barton, Chem. Commun. 49 (2013) 3617-3630.

[6] N.P. E. Barry, P.J. Sadler, Chem. Commun. 49 (2013) 5106-5131.

[7] G.S. Smith, B. Therrien, Dalton Trans. 40 (2011) 10793-10800.

[8] C.G. Hartinger, N. Metzler-Nolte, P.J. Dyson, Organometallics, 31 (2012) 5677-5685.

[9] G. Gasser, I. Ott, N. Metzler-Nolte, J. Med. Chem. 54 (2011) 3-25.

[10] T. Gianferrara, I. Bratsos, E. Alessio, Dalton Trans. 37 (2009) 7588–7598.

[11] C.G. Hartinger, P.J. Dyson, Chem. Soc. Rev. 38 (2009) 391–401.

[12] N. Muhammad, Z. Guo, Curr. Opin. Chem. Biol. 19 (2014) 144-153.

[13] G. Sava, A. Bergamo, In: A. Bonetti, R. Leone, F.M. Muggia, S.B. Howell (eds) Platinum and other heavy metal compounds in cancer chemotherapy. Humana Press, Totowa, 2009, pp 57–66.

[14] D.S. Thompson, G.J. Weiss, S.F. Jones, H.A. Burris, R.K. Ramanathan, J.R. Infante, J.C. Bendell, A. Ogden, D.D. Von Hoff, J. Clin. Oncol. 2012, 30 (suppl; abstr 3033).

ACCEPTED MANUSCRIPT

[15] U. Schatzschneider, J. Niesel, I. Ott, R. Gust, H. Alborzinia, S. Wölfl, ChemMedChem, 3 (2008) 1104-1109.

[16] H.Y. Huang, P.Y. Zhang, B.L. Yu, Y. Chen, J.Q. Wang, L.N. Ji, H. Chao, J. Med. Chem. 57 (2014) 8971-8983.

[17] B. Peña, A. David, C. Pavani, M.S. Baptista, J.P. Pellois, C. Turro, K.M. Dunbar, Organometallics, 33 (2014) 1100-1103.

[18] G.B. Jiang, J.H. Yao, J. Wang, W. Li, B.J. Han, Y.Y. Xie, G.J. Lin, H.L. Huang, Y.J. Liu, New J Chem. 38 (2014) 2554-2563.

[19] S.H. Lai, G.B. Jiang, J.H. Yao, W. Li, B.J. Han, C. Zhang, C.C. Zeng, Y.J. Liu, J. Inorg. Biochem. 152 (2015) 1-9.

[20] M. Yamada, Y. Tanaka, Y. Yoshimoto, S. Kuroda, I. Shimao, Bull. Chem. Soc. Jpn. 65 (1992) 1006-1011.

[21] B.P. Sullivan, D.J. Salmon, T.J. Meyer, Inorg. Chem. 17 (1978) 3334-3341.

[22] J.P. Collin, J.P. Sauvage, Inorg. Chem. 25 (1986) 135–141.

[23] T. Mosmann, J. Immunol. Methods. 65 (1983) 55-63.

[24] K.K. Lo, T.K. Lee, J.S. Lau, W.L. Poon, S.H. Cheng, Inorg. Chem. 47 (2008) 200-208.

[25] S.H. Lai, W. Li, J.H. Yao, B.J. Han, G.B. Jiang, C. Zhang, C.C. Zeng, Y.J. Liu, J. Photochem & Photobiol B: Biology, 158 (2016) 39-48.

[26] Q. Chen, J.Q. Wang, C.L. Song, L.L. Wang, L.N. Ji, H. Chao, Metallomics, 5 (2013) 844-854.

[27] C.C. Zeng, S.H. Lai, J.H. Yao, C. Zhang, H. Yin, W. Li, B.J. Han, Y.J. Li, Eur. J.

ACCEPTED MANUSCRIPT

Med. Chem. 122 (2016) 118-126.

[28] C. Alapetite, T. Wachter, E. Sage and E. Moustacchi, Int. J. Radiat. Biol. 69 (1996) 359-369.

[29] H.U. Simon, A. Haj-Yehia, F. Levi-Schaffer, Apoptosis, 5 (2000) 415-418.

[30] E. Cadenas, K.J.A. Davies, Free Radical Biol. Med. 29 (2000) 222-230.

[31] Z.D. Luo, L.L. Yu, F. Yang, Z.N. Zhao, B. Yu, H.Q. Lai, K.H. Wong, S.M. Ngai, W.J. Zheng, T.F. Chen, Metallomics, 6 (2014) 1480-1490.

[32] Y. Chen, M.Y. Qin, L. Wang, H. Chao, L.N. Ji, A.L. Xu, Biochimie, 95 (2013) 2050-2059.

[33] W. Li, B.J. Han, J.H. Yao, G.B. Jiang, Y.J. Liu, RSC Adv. 5 (2015) 24534-24543.

[34] A. Kawiak, J. Zawacka-Pankau, A. Wasilewska, G. Stasilojc, J. Bigda, E. Lojkowska, J. Nat. Prod. 75 (2012) 9-14.

[35] L.R. Silveira, L. Pereira-Da-Silva, C. Juel, Y. Hellsten, Free Radic. Biol. Med. 35 (2003) 455-464.

[36] T.F. Chen, Y.S. Wong, Int. J. Biochem. Cell Biol. 41 (2009) 666-676.

[37] T.F. Chen, Y.S. Wong, Cell. Mol. Life Sci. 65 (2008) 2763-2775.

[38] M. Giorgio, E. Migliaccio, F. Orsini, D. Paolucci, M. Moroni, C. Contursi, G. Pelliccia, L. Luzi, S. Minucci, M. Marcaccio, P. Pinton, R. Rizzuto, P. Bernardi, F. Paolucci, P.G. Pelicci, Cell, 122 (2005) 221-233.

[39] G. Marverti, A. Ligabue, M. Montanari, D. Guerrieri, M. Cusumano, M. Pietro, L. Troiano, E. Vono, S. Iotti, G. Farruggia, F. Wolf, M. Monti and C. Frassineti,

ACCEPTED MANUSCRIPT

Invest. New Drugs, 29 (2011) 73-86.

[40] A.L. Wang, M.E. Boulton, W.A. Dunn, H.V. Rao, J. Cai, T.J. Lukas, A.H. Neufeld, Autophagy, 5 (2009) 1190-1193.

[41] G.S. Salvesen, V.M. Dixit, Cell, 91 (1997) 443-446.

[42] N.A. Thornberry, Y. Lazebnik, Science, 281 (1998) 1312-1316.

[43] N.N. Danial, S.J. Korsmeyer, Cell, 116 (2004) 205-219.

[44] H. Thomadaki, A. Scorilas, Crit. Rev. Clin. Lab. Sci. 43 (2006) 1-67.

ACCEPTED MANUSCRIPT

ACCEPTED MANUSCRIPT

Captions for Schemes and Figures

Table 1 The IC_{50} values (μM) of ligand and the complexes toward the selected cell lines

Scheme 1 Structures of Ru(II) dppz-like complexes

Fig. 1 BEL-7402 cells were stained with AO/EB and observed under fluorescent microscope. BEL-7402 (a) exposed to 6.25 μM of complexes **1** (b), **2** (c), **3** (d), **4** (e), **5** (f) and **6** (h) for 24 h.

Fig. 2 Comet assay of EB-stained BEL-7402 cells (a) exposure to 6.25 μM of complexes **1** (b), **2** (c), **3** (d), **4** (e), **5** (f) and **6** (g) for 24 h.

Fig. 3 (A) Intracellular ROS was detected in BEL-7402 cells (a) exposure to Rosup (b, positive control) and 6.25 μM of complexes **1** (c), **2** (d) , **3** (e), **4** (f), **5** (g) and **6** (h) for 24 h. (B) The DCF fluorescent intensity was determined by flow cytometry after BEL-7402 (a) cells were exposed to 6.25 μM of complexes **1** (b), **2** (c), **3** (d), **4** (e), **5** (f) and **6** (g) for 24 h. I stands for the fluorescent intensity.

Fig. 4 (A) Assay of BEL-7402 cells mitochondrial membrane potential with JC-1 as fluorescent probe. BEL-7402 cellv (a) exposed to cccp (b, positive control) and 6.25 μM of complexes **1** (c), **2** (d), **3** (e), **4** (f), **5** (g) and **6** (h) for 24 h. (B) The ratio (R) of red/green fluorescent intensity was determined by flow cytometry after BEL-7402 cells were treated with 6.25 μM of complexes **1**-**6** for 24 h.

Fig. 5 Cell cycle distribution of BEL-7402 cells exposure to 6.25 μM of complexes

ACCEPTED MANUSCRIPT

1-**6** for 24 h.

Fig. 6 (A) Microscope images of invading BEL-7402 cells (a) that have migrated through the Matrigel induced by 6.25 μM of complexes **1** (b), **2** (c), **3** (d), **4** (e), **5** (f) and **6** (g) for 24 h.

Fig. 7 BEL-7402 cells were treated with 6.25 μM of the complexes for 24 h and the expression levels of caspases and Bcl-2 family proteins were examined by western blot.

ACCEPTED MANUSCRIPT

ACCEPTED MANUSCRIPT

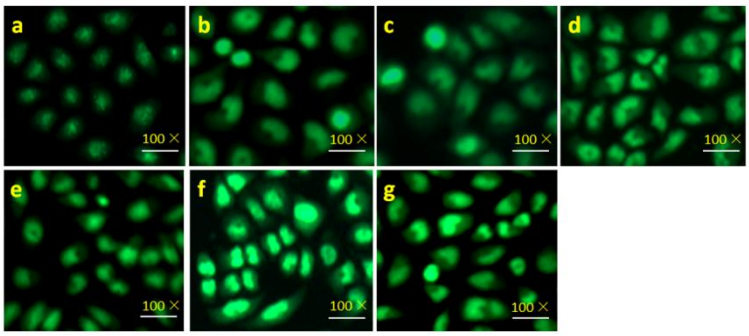

Fig. 1 BEL-7402 cells were stained with AO/EB and observed under fluoresent microscope. BEL-7402 cells (a) were exposed to 6.25 μM of complexes **1** (b), **2** (c), **3** (d), **4** (e), **5** (f) and **6** (g) for 24 h.

ACCEPTED MANUSCRIPT

ACCEPTED MANUSCRIPT

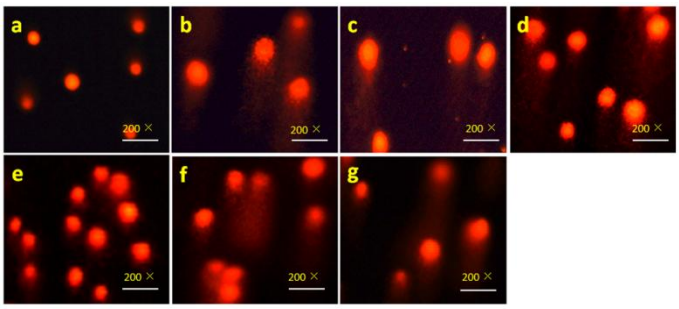

Fig. 2 Comet assay of EB-stained BEL-7402 cells (a) exposure to 6.25 μM of complexes **1** (b), **2** (c), **3** (d), **4** (e), **5** (f) and **6** (g) for 24 h.

ACCEPTED MANUSCRIPT

ACCEPTED MANUSCRIPT

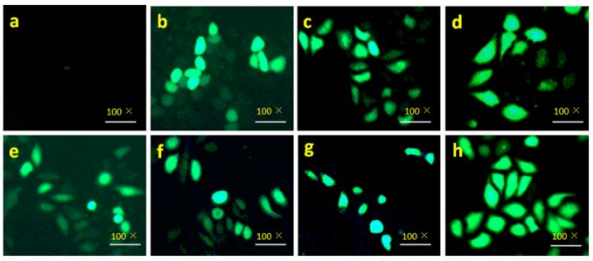

Fig. 3 (A) Intracellular ROS was detected in BEL-7402 cells (a) exposure to Rosup (b) and 6.25 μM of complexes **1** (c), **2** (d) , **3** (e), **4** (f), **5** (g) and **6** (h) for 24 h. Rosup was used as positive control.

ACCEPTED MANUSCRIPT

ACCEPTED MANUSCRIPT

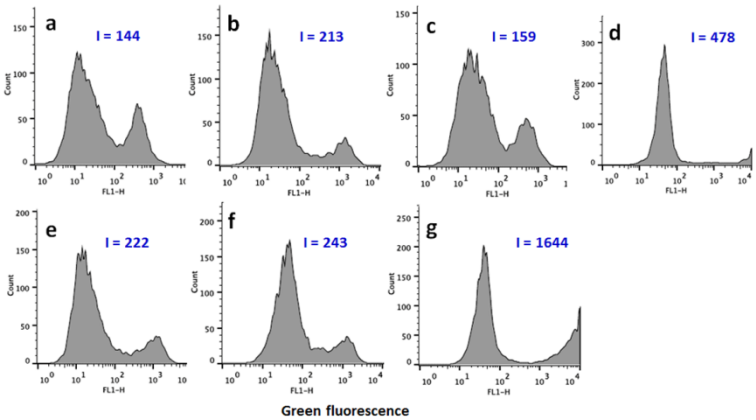

Fig. 3B The DCF fluorescent intensity was determined by flow cytometry after BEL-7402 (a) cells were exposed to 6.25 μM of complexes **1** (b), **2** (c), **3** (d), **4** (e), **5** (f) and **6** (g) for 24 h. I stands for the fluorescent intensity.

ACCEPTED MANUSCRIPT

ACCEPTED MANUSCRIPT

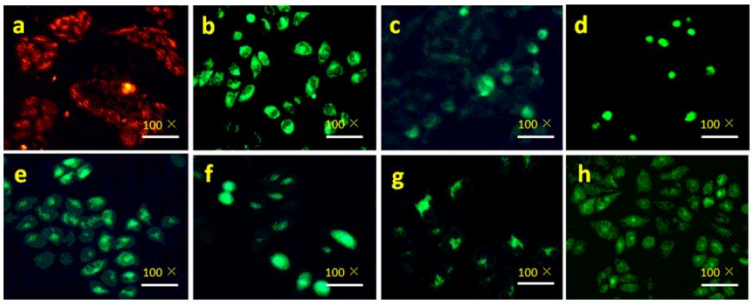

Fig. 4A Assay of BEL-7402 cells mitochondrial membrane potential with JC-1 as fluorescent probe. BEL-7402 cellv (a) exposed to cccp (b, positive control) and 6.25 μM of complexes **1** (c), **2** (d), **3** (e), **4** (f), **5** (g) and **6** (h) for 24 h.

ACCEPTED MANUSCRIPT

ACCEPTED MANUSCRIPT

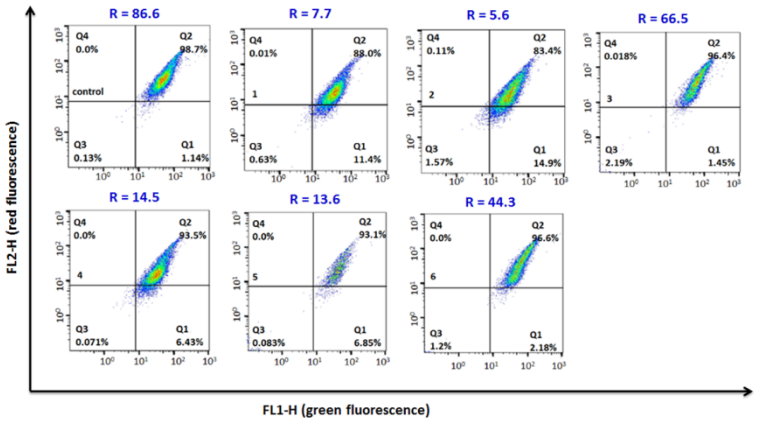

Fig. 4B The ratio of red (FL2-H)/green (FL1-H) after BEL-7402 cells were treated with 6.25 μM of complexes **1-6** for 24 h.

ACCEPTED MANUSCRIPT

ACCEPTED MANUSCRIPT

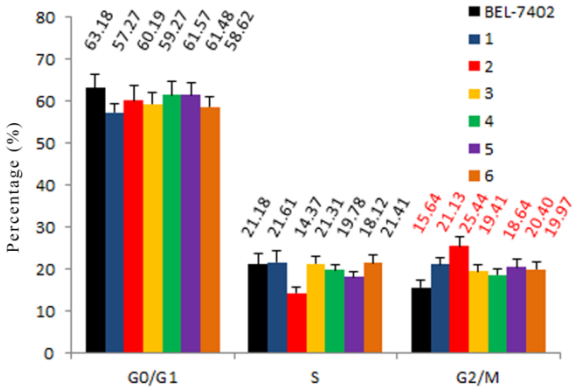

Fig.5 Cell cycle distribution of BEL-7402 cells exposure to 6.25 μM of complexes **1-6** for 24 h.

ACCEPTED MANUSCRIPT

ACCEPTED MANUSCRIPT

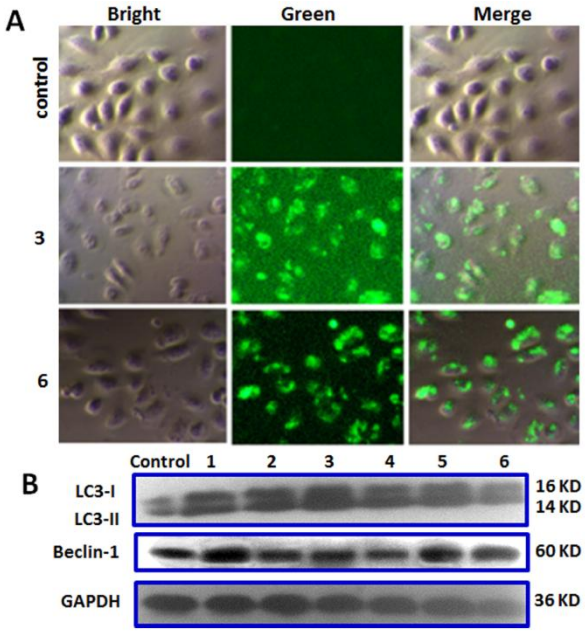

Fig. 6 (A) Autophagy in BEL-7402 cells induced by 6.25 μM of complexes 3 and 6 for 24 h. Autophagy was assayed with MDC staining. (B) The assay of LC3 and Beclin-1 proteins by western blot.

ACCEPTED MANUSCRIPT

ACCEPTED MANUSCRIPT

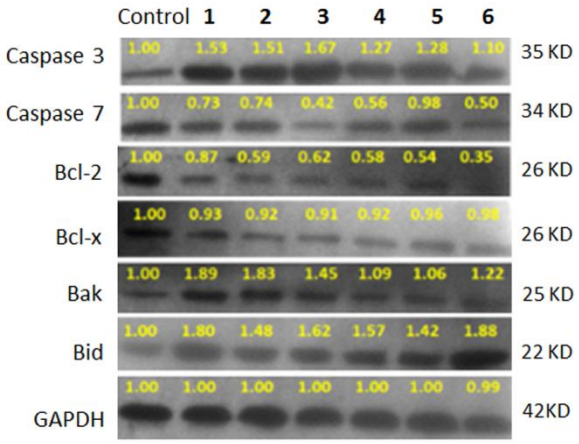

Fig. 7 BEL-7402 cells were treated with 6.25 μM of the complexes for 24 h and the expression levels of caspases and Bcl-2 family proteins were examined by western blot.

ACCEPTED MANUSCRIPT

ACCEPTED MANUSCRIPT

Table 1 The IC_{50} (μM) values of complexes **1-6** toward the selected cell lines

Comp	HeLa	BEL-7402 48 h	BEL-7402 24 h	A549	HepG-2	HOS	LO2
1	13.9 ± 1.0	19.8 ± 5.0	70.6 ± 4.4	16.8 ± 0.8	23.1 ± 1.3	11.0 ± 0.5	37.1 ± 3.3
2	4.1 ± 0.3	2.2 ± 0.2	78.2 ± 3.5	24.8 ± 8.6	2.0 ± 0.2	19.9 ± 0.7	29.9 ± 4.5
3	6.3 ± 0.2	1.5 ± 0.1	14.4 ± 0.8	15.8 ± 0.2	11.6 ± 1.1	4.9 ± 1.6	7.6 ± 0.2
4	55.9 ± 7.5	11.9 ± 2.0	127.0 ± 8.6	26.0 ± 5.7	9.8 ± 0.9	20.7 ± 0.1	52.9 ± 6.9
5	10.0 ± 0.7	6.1 ± 0.6	35.6 ± 1.6	2.5 ± 0.6	3.7 ± 0.3	2.6 ± 0.1	12.9 ± 1.7
6	6.7 ± 1.4	3.2 ± 0.1	12.8 ± 0.4	8.2 ± 0.4	5.6 ± 0.9	4.9 ± 0.2	2.1 ± 0.1
Cisplatin	7.3 ± 1.4	11.5 ± 1.3	nd	7.5 ± 1.3	11.5 ± 1.2	nd	9.3 ± 1.5

nd = not determined

ACCEPTED MANUSCRIPT

ACCEPTED MANUSCRIPT

Table 2 The number of cell invasion and inhibition percentage of cell invasion by 6.25 μM of complexes **1**-**6**.

complex	control	**1**	**2**	**3**	**4**	**5**	**6**
Invasion cells number	363	286	290	285	275	261	241
Inhibition percentage (%)		21.2	20.1	21.5	25.3	28.1	33.6

ACCEPTED MANUSCRIPT

ACCEPTED MANUSCRIPT

Table 3 Inhibition percentage of cell invasion by different concentration of complex **6**

Concentration (μM)	6.25	12.5	25.0	50.0
Inhibition percentage (%)	33.6	38.3	43.5	58.5

ACCEPTED MANUSCRIPT

ACCEPTED MANUSCRIPT

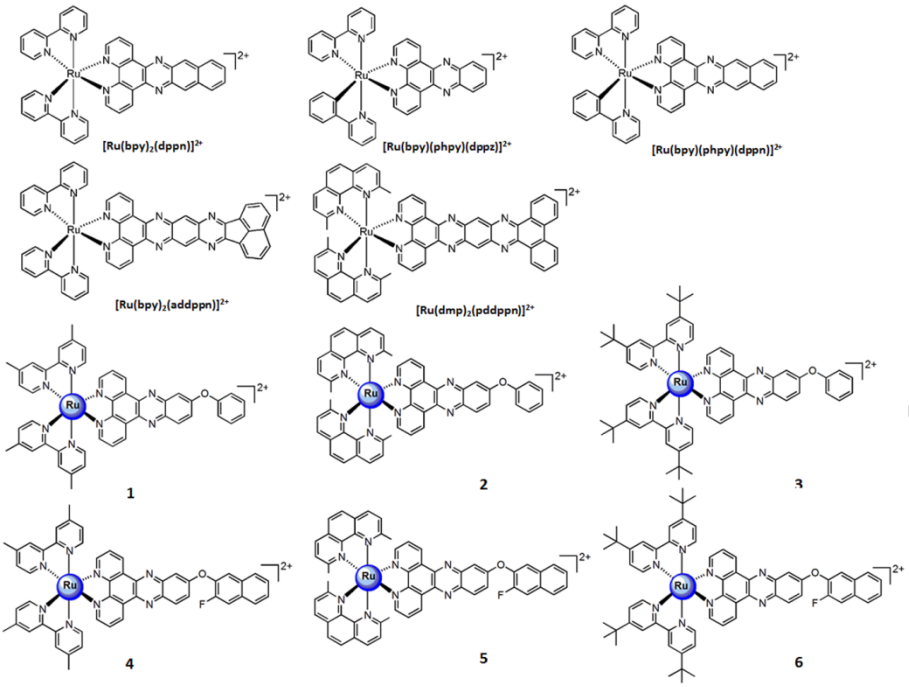

Scheme 1 Structures of Ru(II) dppz-like complexes

ACCEPTED MANUSCRIPT

ACCEPTED MANUSCRIPT

Graphical abstract

Six new ruthenium(II) polypyridyl complexes were synthesized and characterized in detail. The anticancer activity was investigated by cytotoxicity in vitro, apoptosis, reactive oxygen species (ROS), mitochondrial membrane potential, cell cycle arrest, cell invasion, autophagy and proteins expression.

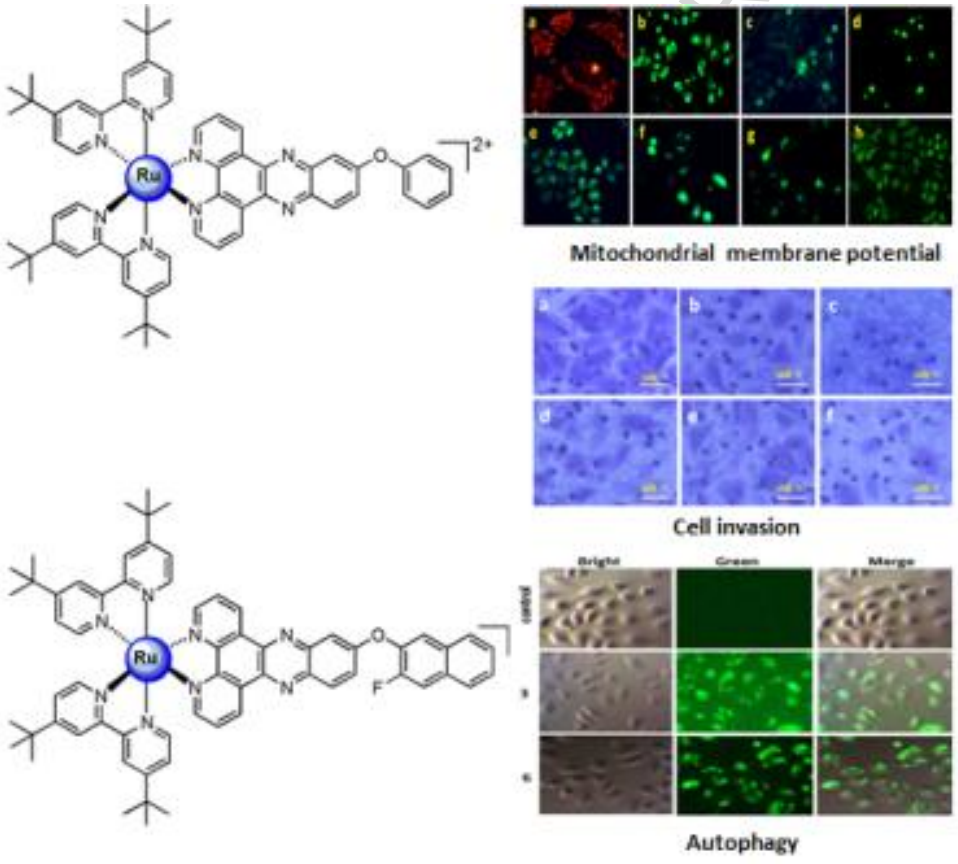

ACCEPTED MANUSCRIPT

Highlights

- Six new ruthenium (II) complexes were synthesized and characterized.
- The cytotoxicity was evaluated by 3-(4,5-dimethylthiazole)-2,5-diphenyltetraazolium bromide method.
- The apoptosis, comet assay, reactive oxygen species and cell invasion were investigated.
- The mitochondrial membrane potential and cell cycle arrest were assayed.
- The expression of caspases and B-cell lymphoma-2 proteins was studied by western blot.

ACCEPTED MANUSCRIPT